GEOPHYSICAL RESEARCH LETTERS, VOL. 36, L06810, doi:10.1029/2009GL037174, 2009

Decadal change in intraseasonal variability over the South China Sea

Yoshiyuki Kajikawa,[1] Tetsuzo Yasunari,[2] and Bin Wang[1,3]

Received 5 January 2008; revised 20 February 2009; accepted 24 February 2009; published 27 March 2009.

[1] Evidence is presented to reveal a decadal change around mid-1990s in the behavior of intraseasonal variability (ISV) over the South China Sea (SCS). During 1979–1993, the ISV has a spectral peak around 64 days, which is longer than in the recent epoch of 1994–2007 (around 42 days). The ISV event in 1979–1993 involves a merging process of the northward and westward propagating convection anomalies over the western North Pacific. The ISV in 1994–2007 has no such a merging process but exhibits a tilted band structure extending from the northern Indian Ocean to the SCS, which is strongly connected to the equatorial eastward propagating Madden-Julian Oscillation. The merging process during 1979–1993 modified the ISV over the SCS, resulting in the prolonged period, enhanced convective activity and a weakened relationship with the eastward propagating MJO. The possible cause of this change is discussed. **Citation:** Kajikawa, Y., T. Yasunari, and B. Wang (2009), Decadal change in intraseasonal variability over the South China Sea, *Geophys. Res. Lett.*, *36*, L06810, doi:10.1029/2009GL037174.

1. Introduction

[2] The South China Sea summer monsoon (SCSSM) is an important component of the Asian summer monsoon. After the discovery of the eastward propagating Madden-Julian Oscillation (MJO) [*Madden and Julian*, 1972], the active/break cycle of the Asian summer monsoon have been recognized as a results of northward propagation of the intraseasonal convection system [*Yasunari*, 1980, 1981], which is sometimes but not always linked to the MJO [*Wang and Rui*, 1990]. The SCSSM has strongest intraseasonal variability (ISV) over the entire Asian summer monsoon regions [*Kemball-Cook and Wang*, 2001]. Furthermore, the ISV over the South China Sea (SCS) has relatively large interannual variability compared with those over the Arabian Sea and the Bay of Bengal [*Kajikawa and Yasunari*, 2005]. Better understand the behavior of the SCSSM system is important as it can affect the weather and climate over the East Asia [*Nitta*, 1987], Indo-China, the western North Pacific and even the Indian Ocean and maritime continent [*Kajikawa et al.*, 2003].

[3] Previous studies have described the mean temporal evolution of the ISV over the Indian Ocean and western North Pacific. Some differences were found in the composite spatial structure of the ISV. For instance, using OLR data for the period 1974–1997, *Goswami and Mohan* [2001] showed that the ISV based on convection anomalies over the Bay of Bengal has a zonally elongated structure of convection anomalies across the northern Indian Ocean and western North Pacific. On the other hand, using OLR data for the period 1979–1993, *Hsu and Weng* [2001] showed a quadrapole structure of convection anomalies, which are zonally out of phase between the northern Indian Ocean and the western North Pacific. This discrepancy could be due to their data covering different periods but could also arise from the non-stationary behavior of the ISV.

[4] *Kwon et al.* [2005] found a significant decadal change in the relationship between the East Asian monsoon and the western North Pacific monsoon before and after (inclusive) 1994. *Kwon et al.* [2007] also discussed the climate shift of summertime circulation over the East Asia and suggested that the increasing the number of typhoon in the western North Pacific may have impacted the precipitation increase over the southern China since the mid-1990s. This decadal shift also induced the decadal change of the SCSSM [*Wang et al.*, 2009] and potentially the ISV over the SCS.

[5] Therefore, this study investigates the possible long-term change of the ISV properties over the SCS with a special focus on periodicity and spatial-temporal evolution during the 29 years from 1979 to 2007. The data used herein include daily interpolated outgoing longwave radiation (OLR) from the NOAA satellite [*Liebmann and Smith*, 1996] and the wind data from the NCEP/NCAR reanalysis project [*Kalnay et al.*, 1996].

2. Decadal Change in Temporal Characteristics

[6] First, we applied the Morlet wavelet analysis to original daily OLR data averaged over the northern SCS (110°E–120°E, 10°N–20°N) for highlighting the interannual and interdecadal features of the convective activity. Figure 1 shows the wavelet power that is significant above 95% confidence level for red noise. On the ISV (30-70-day) time scale, the wavelet power is remarkable during boreal summer of 1979, 1980, 1984, 1985, 1988, 1994, 1996, 1998, 2000, 2001, 2002, 2005, 2006 and 2007. It is of interest to note that the wavelet power for active ISV in 1980s shows a significant peak that extends to beyond 60 days; in contrast, the significant wavelet peak after 1990 occurs on a time scale shorter than 60 days. This calls the decadal change of the ISV between 1988 and 1994. Considering the climate shift over the East Asia and western North Pacific in 1993/1994 by *Kwon et al.* [2005, 2007], it is suggested that this periodicity difference in the ISV over the SCS is possibly associated with the decadal change in mid-1990s. Therefore, we decide to look into changes of the ISV behavior before and after (inclusive) 1994.

[7] In order to verify the decadal change of the ISV over the SCS, we first applied the spectrum analysis to original

[1]International Pacific Research Center, University of Hawai'i at Manoa, Honolulu, Hawaii, USA.
[2]Hydrospheric Atmospheric Research Center, Nagoya University, Nagoya, Japan.
[3]Department of Meteorology, University of Hawai'i at Manoa, Honolulu, Hawaii, USA.

0094-8276/09/2009GL037174$05.00

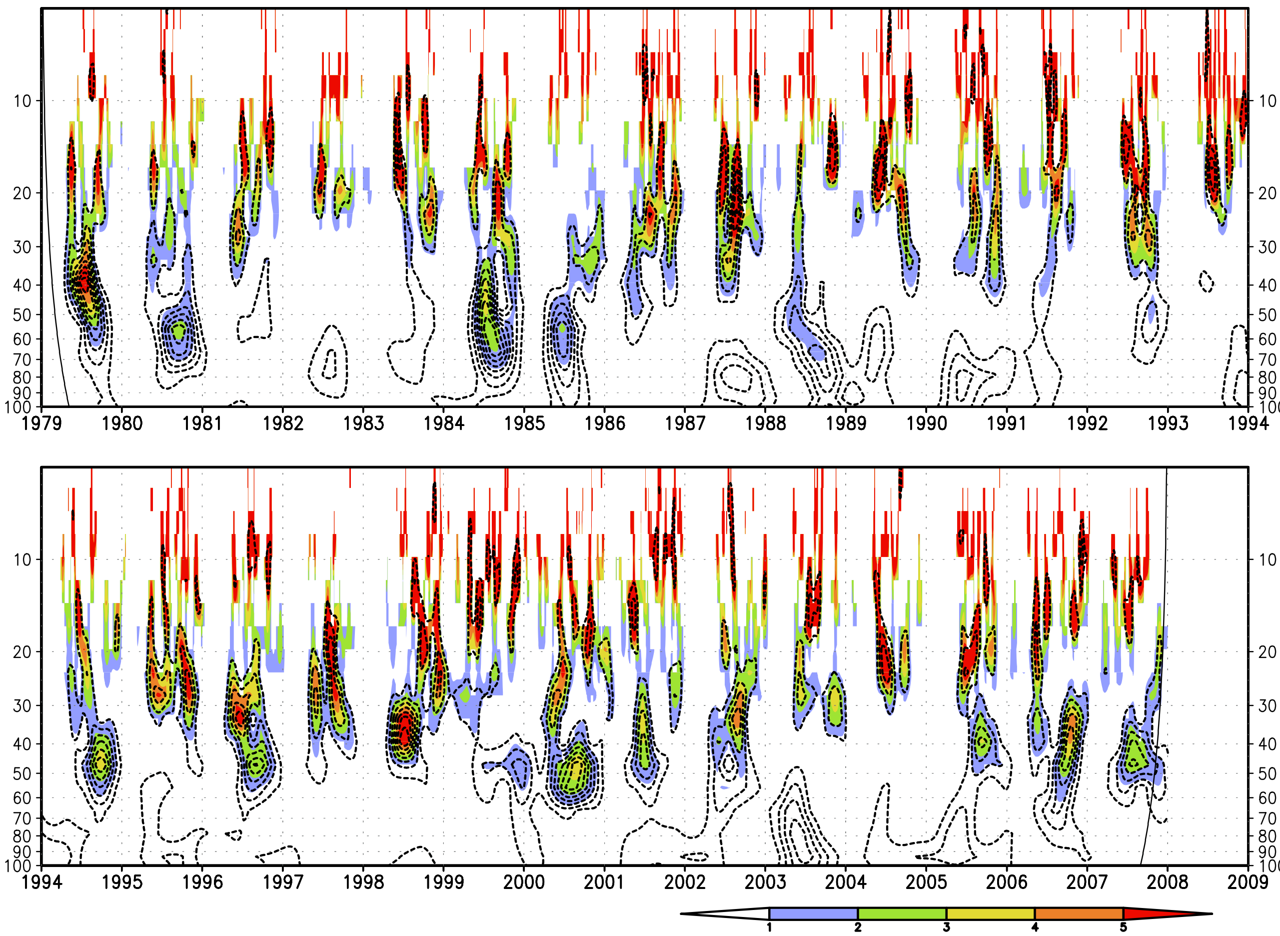

Figure 1. Wavelet power spectrum of daily OLR averaged over the SCS (110°E–120°E, 10°N–20°N) (dashed contour) and the ratio to the wavelet power of the 95% confidence level for red-noise processes (shading). Contour interval is 4.0×10^3 (w^2/m^4).

daily OLR data over the SCS (110°E–120°E, 10°N–20°N) for May–September during 1979–2007. Then, we computed ensemble mean spectrum power for the two epochs: 1979–1993 and 1994–2007. A significant spectral peak at 64 day in 1979–1993 is found in Figure 2a (red line), while the significant peak at 42 day is seen in 1994–2007 (blue line).

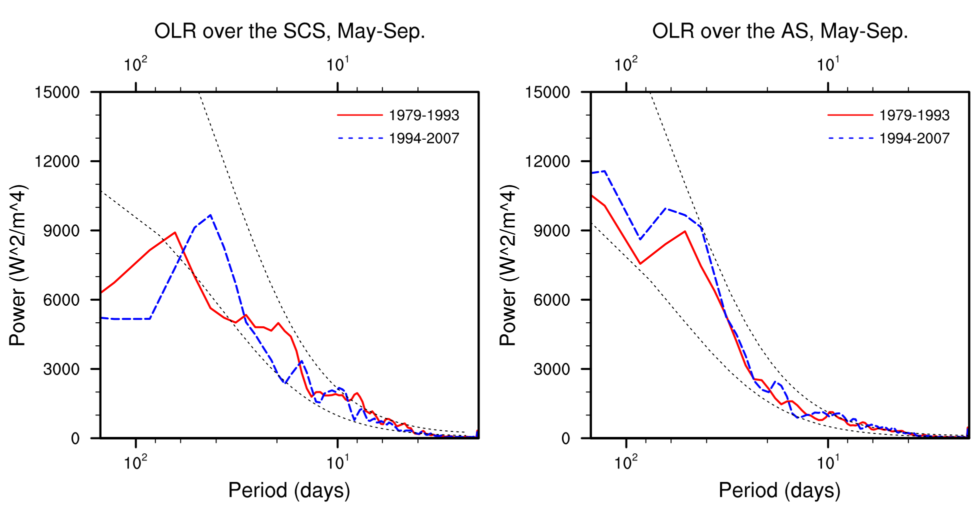

Figure 2. (a) Ensemble power spectrum of daily OLR time series (May to September) averaged over the South China Sea (110°E–120°E, 10°N–20°N) during 1979–1993 (red line) and 1994–2007 (blue dashed line). (b) Same as Figure 2a but for over the Arabian Sea (65°E–75°E, 10°N–20°N). Red Noise spectrum and its 95% confidence level are also shown as dotted line.

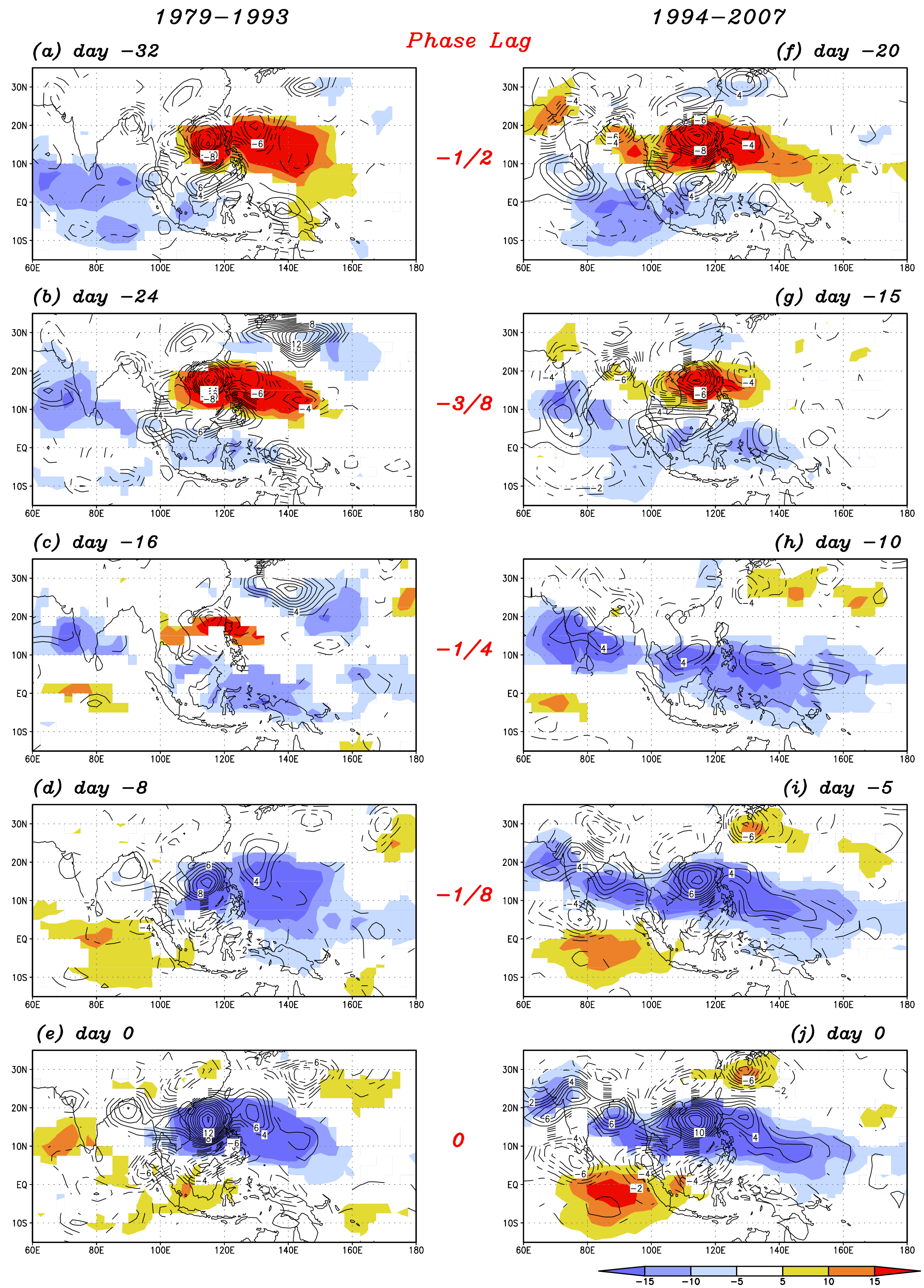
1979–1993
1994–2007
Phase Lag
(a) day −32
(f) day −20
−1/2
(b) day −24
(g) day −15
−3/8
(c) day −16
(h) day −10
−1/4
(d) day −8
(i) day −5
−1/8
(e) day 0
(j) day 0
0
−15 −10 −5 5 10 15

Figure 3

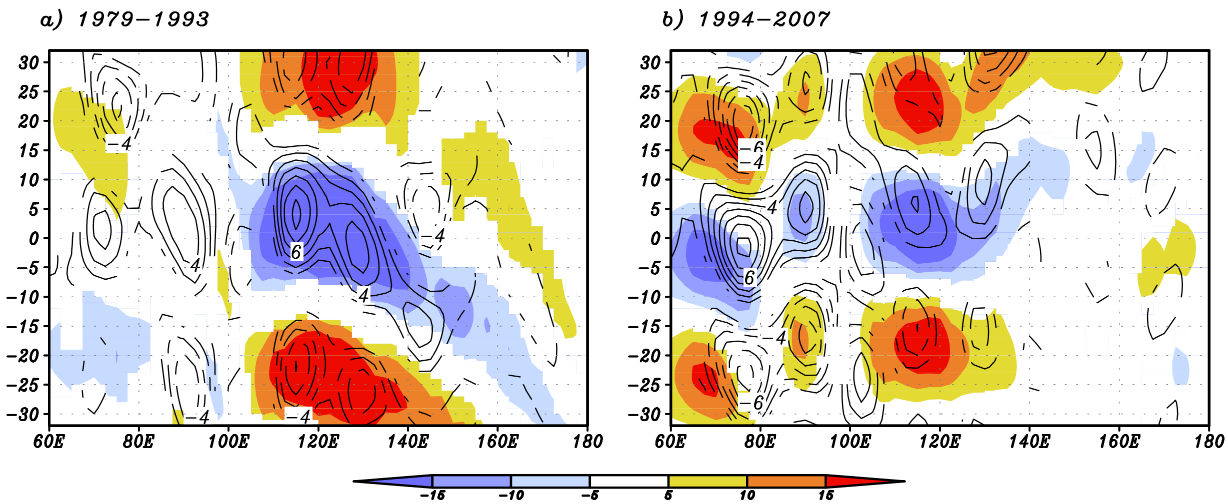

Figure 4. Time-longitude diagram of lag-regression of band-pass filtered anomalies of OLR (Wm^{-2}) along 20°N (shaded) and 850 hPa relative vorticity along 25°N (contour) in (a) 1979–1993 and (b) 1994–2007. All anomalies are plotted in the same manner of Figure 3.

This period difference (about 20 days) is statistically significant between the two epochs. The spectrum difference around 42days is also significant by the Welch's two-sample t-test. In contrast, the spectrum power of OLR over the Arabian Sea (110°E–120°E, 10°N–20°N; Figure 2b) for May–September does not show significant difference between 1979–1993 and 1994–2007. The periodicity of the ISV over the SCS in 1994–2007 is very close to that over the Arabian Sea in 1994–2007, whereas different in 1979–1993. The ensemble mean spectrum over the Bay of Bengal also shows no significant difference between 1979–1993 and 1994–2007 (figure not shown). Thus, it is suggested that the decadal change of the ISV in terms of periodicity occurs only over the SCS and this also implies a change in the spatial structure of the ISV between the two epochs, especially the phase relationship between the SCS and the Arabian Sea/Bay of Bengal.

3. Epochal Differences in the Spatial and Temporal Evolution

[8] Based on the results of the wavelet and spectrum analysis, the band-pass filtering of the data was performed for the entire period by using the 30–80 day Lanczos filter [*Duchon*, 1979] with 121 weights. In order to identify the difference in the spatial-temporal evolution of the ISV between the two epochs, we calculated the lagged regression coefficient between the filtered OLR time series over the SCS (110°E–120°E, 10°N–20°N) and the OLR and 850 hPa relative vorticity anomalies over the entire domain of interest during boreal summer (June–September). Since the periodicity of the ISV is different in the two epochs, we identify eight phases as one cycle of the ISV with the day of maximum convection over the SCS as 0 day in the two epochs respectively. The interval between each phase is 8 days for the epoch 1979–1993 and 5 days for the epoch 1994–2007.

[9] Figure 3 shows the temporal evolution of the ISV for the two epochs from −1/2 cycle (−32 days for the 1979–1993 and −20 days for the 1994–2007) to phase lag 0. The eastward propagating convection along the equator to 10°S and the northward propagating convection over the Arabian Sea and the western North Pacific are seen in both epochs. Also, a positive vorticity anomaly is always located to the northwest of the negative OLR anomaly. In spite of these common features, distinctive ISV evolutions are seen during the two epochs.

[10] During the epoch 1979–1993, a prominent process is the merging the two convection anomalies over the SCS and Philippine Sea. One convection anomaly moves northward from the maritime continent from day −16 to day −8 (Figures 3c–3d), which comes originally from the eastward moving convection anomaly over the equatorial Indian Ocean (Figures 3a–3b). The other is a westward moving convection anomaly over the western North Pacific. This is seen in the northwestern Pacific (150°E, 25°N) in Figures 3a–3b and moves westward accompanied by significant strong cyclonic circulation in transition phase (Figures 3c–3d). It is suggested that the origin of these convection and vorticity anomalies come from the vicinity of the dateline by considering the opposite sign of day −16

Figure 3. Lag-regression of band-pass filtered anomalies of OLR (Wm^{-2}; shaded) and relative vorticity at 850 hPa level (contour) upon the filtered OLR index over the SCS during boreal summer (JJAS) in 1979–1993 from (a) a lag of 1/2 cycle to (e) a day with maximum convection over the SCS with 1/8 cycle interval. Figures 3f–3j are the same as Figures 3a–3e but for 1994–2007. The period of 1/8 cycle is 8 (5) days for the epoch 1979–1993 (1994–2007). The contour interval is 10^{-7} [s^{-1}], and the dashed contour is negative. All anomalies are opposite in sign to original for setting maximum convection peak over the SCS in Figure 3e day 0. The regression coefficients have been multiplied by one standard deviation of band-pass filtered OLR anomalies over the SCS, and only those that are significant at the 95% level by Student's t-test are plotted.

and day −8 (170°E, 25°N) in Figures 3d–3e. These two convection anomalies merge over the SCS and Philippine Sea, and the convection is abruptly strengthened after the merge at day 0 (Figure 3e). Another interesting feature is the out-of-phase convection anomalies between the northern Indian Ocean and SCS. This is also associated with the 'quadrapole' pattern of OLR over the Indian Ocean and the western Pacific in the transition phase day −16, (1/4 phase lag). In addition, the convection anomaly over the Bay of Bengal is not associated with the convection over the SCS during the epoch 1979–1993.

[11] On the other hand, the temporal evolution during the epoch 1994–2007 has no merging process but exhibits a clear west-northwest to east-southeast tilted "band" structure, which extends from the northern Indian Ocean to the western North Pacific. This tilted band structure includes significant anomalies over the Bay of Bengal, where convective anomalies were absent in the epoch 1979–1993. This spatial structure also indicates that the convection anomalies over the northern Indian Ocean and the western North Pacific tend to have the same sign. The elongated structure is originated in the enhanced convection anomalies over the southeastern Indian Ocean at day −20 (Figure 3f). These anomalies are clearer and become stronger than those in 1979–1993. After eastward propagation along the equator, the elongated structure moves northward from day −10 to day 0 (Figures 3h–3j).

[12] Figure 4 shows time-longitude diagram of lag-regression of OLR along 20°N and relative vorticity at 850 hPa along 25°N to further reveal the horizontal structure difference between the two epochs. The westward propagating convection and vorticity from 170°E is prominent only in the epoch 1979–1993. The merging of this westward propagating convection with the northward propagating convection from equatorial area (Figure 3) over the SCS enhance convection and prolong the active convection period in 1979–1993. The OLR anomalies over the northern Bay of Bengal and the Arabian Sea are not clear in 1979–1993. In contrast, coherent signal of OLR anomalies over the Bay of Bengal and the Arabian Sea, which is associated with northward propagation of convection anomalies extending from west-northwest to east-southeast, is clear during the epoch 1994–2007. This elongated structure also extends to 140°E after the convection maximum over the SCS.

4. Summary and Discussions

[13] This study detected a decadal change of the ISV over the SCS in mid-1990s, which are distinctive in the periodicity and the temporal-spatial evolution. The significant difference of the period between the epoch 1979–1993 (peak at 64 day) and the epoch 1994–2007 (peak at 42 day) is found in spectrum analysis. In contrast, the ISV over the Bay of Bengal and Arabian Sea does not show such a decadal change in periodicity. In terms of the mean temporal-spatial evolution of the ISV with respect to the convection over the SCS, four different features between the two epochs are found; (1) the merging process over the Philippine Sea and SCS (2) the west-northwest to east-southeast tilted "band" structure, (3) the phase relationship of convection anomalies between the northern Indian Ocean and the western North Pacific, and (4) the convection anomalies over the Bay of Bengal. The merging process of the northward propagating convection from the maritime continent and the westward propagating convection along 20°N–25°N from the central North Pacific is evident only in 1979–1993. The existence of this westward propagation of OLR and vorticity anomalies is consistent with the results by *Hsu and Weng* [2001]. They used OLR data from 1979 to 1993 and pointed out that this merging process may reflect an interaction between the tropics and subtropics. The tilted band structure of OLR and relative vorticity anomalies in the west-northwest to east-southeast direction can be seen only during the epoch 1994–2007 (Figures 3f–3j). This structure resembles closely to the composite structure based on eastern equatorial Indian Ocean convective anomalies derived by *Wang et al.* [2006], who used the TRMM data for the period of 1997–2005. *Waliser et al.* [2004] also showed similar results by using the rainfall data from 1979 to 1999 and extended empirical orthogonal function analysis. The convection anomalies between the northern Indian Ocean and the western North Pacific are in (out of) phase during the epoch 1979–1993 (1994–2007). The quadrapole pattern of OLR anomaly in the transition phase during the epoch 1979–1993 (Figure 3c) is similar to that described by *Annamalai and Slingo* [2001], who used OLR data from 1979 to 1995. The convection anomalies over the Bay of Bengal are strongly connected with that over the SCS as part of an elongated spatial structure only in the epoch of 1994–2007.

[14] The ISV over the over the Arabian Sea and Bay of Bengal has 40-day period during both two epochs (Figure 2), and the periodicity of the ISV over the SCS is close to it during 1994–2007. Furthermore, this period is close to typical eastward propagating global MJO signal. Therefore, the ISV over the SCS during the epoch of 1994–2007 has stronger connection with the MJO signal (e.g. velocity potential at 200 hPa) than during 1979–1993 (figure not shown). Thus, it is suggested that the northward propagating convection system of the Asian monsoon must be associated with the eastward propagating MJO along the equatorial Indian Ocean. However, the westward propagation over the western North Pacific was strongly connected with the northward propagation from the maritime continent during the epoch of 1979–1993. This merging process enhanced the cyclonic circulation over the SCS and enhanced southwesterly embedded in the cyclonic circulation transported more moisture in to the SCS and Philippine Sea [*Hsu and Weng*, 2001]. This could create favorable condition of deep convection longer and inhibited northward propagation from the equator. The ISV over the SCS during 1979–1993 was modified with a prolonged periodicity. In other words, the merge of tropical convection with subtropical convection becomes weak or disappears in recent decades. Since the periodicity of the ISV over the Arabian Sea and Bay of Bengal does not change in the two epochs, this merging process also weakens the relationship between SCS and northern Indian Ocean in the ISV time scale.

[15] Although this study indicates possible decadal change of the ISV over the SCS, it leaves several interesting questions unanswered. More examinations are needed to address the following interesting issues: What is the detailed process of westward propagating convection along 20°N–

25°N? How is the quadrapole structure in 1979–1993 formed? And why is the merging process prominent in 1979–1993? The convection anomalies over the southeastern Indian Ocean and the Bay of Bengal might be an important area for the decadal change of the ISV structure. The SST anomalies over the mid-western Pacific could be associated with the existence of the westward propagating convection and worthwhile to research for addressing above questions.

[16] **Acknowledgments.** The authors acknowledge support from the International Pacific Research Center (IPRC). Bin Wang acknowledges the support by the Climate Dynamics Program of the National Science Foundation and the NOAA OGP through CLIVAR Program. This research was supported by the JAMSTEC, which sponsors research at the IPRC. IPRC/SOEST publication 598/7659.

References

Annamalai, H., and J. Slingo (2001), Active/break cycles: Diagnosis of the intraseasonal variability of the Asian summer monsoon, *Clim. Dyn.*, *18*, 85–102.

Duchon, C. E. (1979), Lanczos filtering in one and two dimensions, *J. Appl. Meteorol.*, *18*, 1016–1022.

Goswami, B. N., and R. S. A. Mohan (2001), Intraseasonal oscillations and interannual variability of the Indian summer monsoon, *J. Clim.*, *14*, 1180–1198.

Hsu, H.-H., and C.-H. Weng (2001), Northward propagation of the intraseasonal oscillation in the western North Pacific during the boreal summer: Structure and mechanism, *J. Clim.*, *14*, 3834–3850.

Kajikawa, Y., and T. Yasunari (2005), Interannual variability of the 10–25- and 30–60-day variation over the South China Sea during boreal summer, *Geophys. Res. Lett.*, *32*, L04710, doi:10.1029/2004GL021836.

Kajikawa, Y., T. Yasunari, and R. Kawamura (2003), The role of the local Hadley circulation over the western Pacific on the zonally asymmetric anomalies over the Indian Ocean, *J. Meteorol. Soc. Jpn.*, *81*, 259–276.

Kalnay, E., et al. (1996), The NCEP/NCAR 40-year reanalysis project, *Bull. Am. Meteorol. Soc.*, *77*, 437–471.

Kemball-Cook, S., and B. Wang (2001), Equatorial waves and air-sea interaction in the boreal summer intraseasonal oscillation, *J. Clim.*, *14*, 2923–2942.

Kwon, M., J.-G. Jhun, B. Wang, S.-I. An, and J.-S. Kug (2005), Decadal change in relationship between east Asian and WNP summer monsoons, *Geophys. Res. Lett.*, *32*, L16709, doi:10.1029/2005GL023026.

Kwon, M., J.-G. Jhun, and K.-J. Ha (2007), Decadal change in east Asian summer monsoon circulation in the mid-1990s, *Geophys. Res. Lett.*, *34*, L21706, doi:10.1029/2007GL031977.

Liebmann, B., and C. A. Smith (1996), Description of a complete (interpolated) outgoing longwave radiation dataset, *Bull. Am. Meteorol. Soc.*, *77*, 1275–1277.

Madden, R. A., and P. R. Julian (1972), Description of global-scale circulation cells in the tropics with a 40–50 day periods, *J. Atmos. Sci.*, *29*, 1109–1123.

Nitta, T. (1987), Convective activities in the tropical western Pacific and their impact on the Northern Hemisphere summer circulation, *J. Meteorol. Soc. Jpn.*, *65*, 373–390.

Waliser, D., R. Murtugudde, and L. E. Lucas (2004), Indo-Pacific Ocean response to atmospheric intraseasonal variability: 2. Boreal summer and intraseasonal oscillation, *J. Geophys. Res.*, *109*, C03030, doi:10.1029/2003JC002002.

Wang, B., and H. Rui (1990), Synoptic climatology of transient tropical intraseasonal convection anomalies, *Meteorol. Atmos. Phys.*, *44*, 43–61.

Wang, B., P. Webster, K. Kikuchi, T. Yasunari, and Y. Qi (2006), Boreal summer quasi-monthly oscillation in the global tropics, *Clim. Dyn.*, *27*, 661–675.

Wang, B., F. Huang, Z. Wu, J. Yang, X. Fu, and K. Kikuchi (2009), Multi-scale climate variability of the South China Sea monsoon: A review, *Dyn. Atmos. Ocean*, in press.

Yasunari, T. (1980), A quasi-stationary appearance of 30 to 40 day period in the cloudiness fluctuation during the summer monsoon over India, *J. Meteorol. Soc. Jpn.*, *58*, 225–229.

Yasunari, T. (1981), Structure of and Indian summer monsoon system with around 40-day period, *J. Meteorol. Soc. Jpn.*, *59*, 336–354.

Y. Kajikawa, International Pacific Research Center, University of Hawai'i at Manoa, 1680 East West Road, Honolulu, HI 96822, USA. (ykaji@hawaii.edu)

B. Wang, Department of Meteorology, University of Hawai'i at Manoa, Honolulu, HI 96822, USA.

T. Yasunari, Hydrospheric Atmospheric Research Center, Nagoya University, Nagoya 464-8601, Japan.